dr inż. Artur Błachowski November 21st 2011

Załącznik 3

AUTOREFERAT
English version

The set of papers declared as habilitation papers consists of fourteen papers concerned with the topic: „Impurity effect on spin and charge density in iron studied by Mössbauer spectroscopy" [1-14]. They are numbered by the date of publication in the journals from the Journal Citation Reports database. Two additional papers [15, 16] are strongly related to the previous papers. Remaining six papers [17-22] deal with the current research and they have significant meaning for my plans of the future scientific activity.

Introduction

The set of papers [1-14] is concerned with the influence of impurities on the hyperfine parameters seen by the iron nucleus embedded in the BCC structure of the α-Fe with the assumption that various impurities substitute iron atoms. The binary alloys have been considered with the relatively low concentration of impurities. Mainly d elements have been used as impurities. Alloys described above are simple enough to obtain some meaningful physical insight. On the other hand, they are base for various steels, and therefore have application significance. The ferromagnetism is preserved at low impurity concentration and the system remains close to the ground magnetic state even at room temperature as the magnetic transition temperature is high for α-Fe and it is not perturbed significantly by addition of impurities at the low concentration level. Hyperfine parameters could be easily measured by means of the 14.41-keV resonant transition in ^{57}Fe, the latter being component of the natural iron distributed randomly among the iron atoms. Subsequently hyperfine parameters could be used to estimate various properties of the alloy under investigation.

There were many attempts in the past to deal with the above problem. However, the approach presented here seems the most comprehensive and free of the superfluous approximations.

Model

The model used to process transmission Mössbauer data is described in detail in Refs [1, 3, 13]. It applies to the spectra obtained in the transmission geometry with the help of the commercial single line source having negligible resonant thickness and emitting unpolarized line. The basic assumptions used within this model are as follows. (1) There is no electric quadrupole interaction induced by the impurity on the iron nucleus. This assumption is well confirmed by the experiment, and this feature follows from the large screening of the additional charge by the conduction band. Hence, one is left with the perturbation of the magnetic hyperfine field and perturbation of the total charge on the iron nucleus as the spectra could be processed as time independent spectra described by the semi-classical Hamiltonian. Due to the fact that spectra are collected at room temperature one can safely assume that ground hyperfine states are almost equally populated. (2) It is assumed that dynamics of the iron atom is not perturbed significantly by the impurity. Such approach is justified by metallic character of the bonding potential as far as the recoilless fraction is considered. Hence, the recoilless fraction is fairly isotropic as one stay within the harmonic limit at room temperature. On the other hand, the second order Doppler shift is already in the high

temperature classical limit at room temperature, and it does not depend on the bonding energy. Hence, impurities affect the isomer shift solely, i.e., the charge (electron) density on the iron nucleus. The isomer shift parameters S could be easily transformed into electron density parameters ρ using the relation $\rho = \alpha^{-1} S$ with $\alpha = -0.291\,\mathrm{mm\,s^{-1}\,a.u.^{3}\,el.^{-1}}$ for this particular resonant transition [U.D. Wdowik, K. Ruebenbauer, Phys. Rev. B **76**, 155118 (2007)]. (3) It is assumed that perturbations to the isomer shift and hyperfine field are additive in the algebraic sense and depend only on the distance from the iron nucleus to the impurity – coordination shell of the resonant nucleus. This assumption follows from the fact that all perturbations occur for the strongly itinerant electrons/holes. It was found experimentally that individual impurities are seen by the iron nucleus either to the second or to the third coordination shell at most, as far as the isomer shift and hyperfine field is considered. More distant impurities could contribute to the constant background. Hence, the model relies on three (two shells) or four (three shells) adjustable parameters for the isomer shift (charge/electron density) and additional three or four parameters for the hyperfine field. The number of shells taken into account is the same for both of above hyperfine parameters, as it is defined by the screening potential of the impurity by the conduction band. The hyperfine field represents electron/hole spin density in this highly metallic system enhanced by the constant core polarization. For high quality spectra the impurity concentration could be obtained from the spectra as well. It remains in good agreement with the independent results confirming reliability and numerical stability of the model.

The best results are obtained for random alloys obtained by quench from the liquid state. For high impurity concentration one can expect departure from the simple model outlined above due to the impurity-impurity interaction and inhomogeneity of the alloy. Some alloys are hard to make from the liquid state (Fe-Zn: Ref. [13]) due to the very high vapor pressure of the impurity component or due to the very low solubility of the impurity (Fe-Cu: Ref. [R]). For such systems some ordering of the impurity could occur. There are again many approaches to this problem in the literature. Some of them are very sophisticated and rely on multiple adjustable parameters. It is really impossible to get full information about alloy order from the Mössbauer spectra, as the Mössbauer spectroscopy is a local method. For random alloy a probability to find impurity at particular lattice vortex equals impurity concentration. This probability could be modified by introduction of the order parameters for subsequent coordination shells as the cubic symmetry assures that all vortices of the particular shell are equivalent each other. The model has been extended along this line of reasoning [13]. Usually, the additional constraint is imposed to get reliable results. Namely, it is requested that the average concentration over individual shells seen by the iron nucleus equal the impurity concentration within the alloy. This is quite natural assumption as the number of particles is strictly conserved here. Above average concentration could be set in principle as the adjustable parameter, of course. Application of the particle conservation principle leads to the single order parameter in the case of two distinguished coordination shells. A single order parameter is obtained for the three-shell model provided one assumes additionally that the impurity concentration varies only between two simple cubic sub-lattices composing the BCC lattice. This is again a natural assumption as all vortices of the particular sub-lattice are equivalent each other.

The model has been implemented in the data processing application GMBERNZ belonging to the Mosgraf (Mosgraf-2009) suite available at: www.elektron.up.krakow.pl/mosgraf-2009

Data could be processed in the transmission integral approximation with the complete correction for the polycrystalline absorber thickness. Eventual orientation of crystallites could

be taken into account. All configurations of the impurities within distinguished coordination shells are taken into account. This is extremely important feature as neglected configurations despite low particular probabilities could amount to significant fraction, as they are numerous. In order to neglect them one has to have very small impurity concentration. On the other hand, one cannot decide *a priori* which configurations are negligible while evaluating order parameter(s). Inclusion of subsequent configurations with the increasing impurity concentration makes the whole set of results inconsistent.

Ab initio calculations

In order to obtain reliable hyperfine parameters like the electron density on the nucleus and hyperfine field one has to apply methods designed for the crystalline matter in the case of Mössbauer spectroscopy. All methods yielding trustworthy results rely on the super-cell concept with the periodic boundary conditions. Hence, they are difficult to apply to the more or less random alloy having significant impurity concentration. However, one can study perturbations around isolated impurity quite reliable. Results of calculations have been published in [11, 12, 14]. Calculations were performed within the density functional theorem applying full potential method with the scalar relativistic approach. Orbital terms (full relativistic approach) have been neglected outside the core regions, as systems investigated are highly metallic with negligible orbital contributions due to the conduction bands. On the other hand, inclusion of the itinerant orbital terms is likely to lead to the numerical instabilities for the cases with the almost absent such terms. Electrons were divided according to the binding energy criterion into the core and band electrons. Such simple division leads to greater numerical stability, and there is no need to use semi-core states. A generalized gradient approximation was used, as it is specifically suited for calculations of the hyperfine parameters. The finite size nuclei were used as well. The last point is particularly important for the ^{57}Fe nucleus while calculating electron density in its vicinity. Calculations were performed in two steps. The first step involved radial lattice relaxation (according to the symmetry of the structure) within the hard core approximation, as such approach yields the most reliable structural information. Here the nuclear size does not come into play. Radial relaxation of the structure is small enough to keep the same order of shells as in the pure α-Fe. Relaxed structure was used as input for the all electron application with the proper nuclear radii. The first step was performed by means of the VASP code. The final calculations were performed by the WIEN2k code. Calculations were performed for all d impurities and Ga [14]. Final results were obtained for the 128-atom super-cell with the impurity located in the center. Further details like the choice of the muffin-tin radii, choice of the basal functions, cutoff parameters *etc.* could be found in Ref. [14].

It was found that impurity has twofold effect on the hyperfine interactions, i.e., the volume correction effect and the conduction band modification effect. Note that 3d, 4d and 5d impurities follow the same pattern upon having made the volume correction as shown in Figure 1 reproduced from Ref. [11]. It is strong indication that the band effect is almost the same regardless of the principal quantum number of the d shell of the impurity.

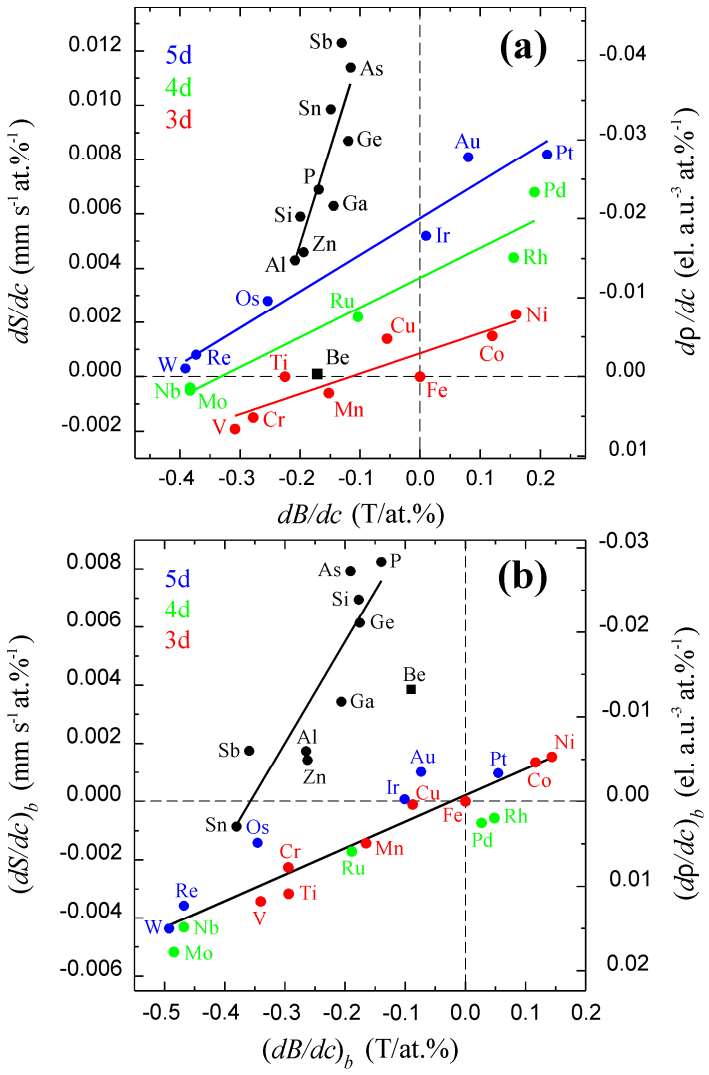

Figure 1 Correlation between electron spin density and electron density variations for various impurities: (a) – total: (b) – volume corrected, i.e., pure band effect. Figure is reproduced from Ref. [11].

Results have been extensively compared with the experimental results obtained by us or taken from the literature. It is surprising that *ab initio* calculations confirmed the simple phenomenological model of Miedema and van der Woude – where applicable. It was confirmed that the iron nucleus sees individual impurities to the third coordination shell at most [14]. A table (reproduced below) giving perturbations caused by individual impurities up to the third coordination shell either to the field or to the electron density on the iron nucleus is compiled in Ref. [14] for all d impurities and Ga. It could be used while seeking order of the alloy or impurity concentration, as the number of adjustable parameters is reduced to the parameters describing effect of the distant impurities. Distant impurities have strong effect in the case of Pd [1] and Ru [4] as far as the electron density on the iron nucleus is considered. This is understandable as the outer electrons of these impurities strongly mix with the conduction band.

Table

(Table is reproduced from Ref. [14])

Perturbations of the electron density $\Delta\rho_s$ and electron spin density ΔB_s on the iron nucleus generated by the single impurity located in subsequent iron coordination shells. Corresponding perturbation of the isomer shift amounts to $\Delta S_s = \alpha\,\Delta\rho_s$ with $\alpha = -0.291\,\mathrm{mm\,s^{-1}\,a.u.^3\,el.^{-1}}$ for the 14.41-keV resonant transition in ^{57}Fe [U.D. Wdowik, K. Ruebenbauer, Phys. Rev. B **76**, 155118 (2007)]. Perturbation ΔB_s directly applies to the iron hyperfine magnetic field. The order of shells remains unperturbed by addition of impurities.

Impurity	$\Delta\rho_1$ (el./a.u.^{3})	$\Delta\rho_2$ (el./a.u.^{3})	$\Delta\rho_3$ (el./a.u.^{3})	ΔB_1 (T)	ΔB_2 (T)	ΔB_3 (T)
Ti	0.072	0.068	0.017	-1.93	-1.92	-0.42
V	0.100	0.050	0.001	-2.05	-2.16	-0.75
Cr	0.108	0.028	0.004	-3.51	-2.86	-0.17
Mn	0.071	0.034	0.005	-2.29	-0.50	0.37
Co	-0.036	-0.040	-0.017	0.56	-0.30	-0.06
Ni	-0.080	-0.076	-0.013	0.20	-0.09	0.22
Cu	-0.098	-0.036	0.014	-0.85	1.00	0.23
Zn	-0.152	-0.050	0.018	-1.34	0.28	-0.74
Ga	-0.195	-0.073	0.016	-1.70	0.21	-1.30
Nb	0.087	0.005	-0.010	-2.10	-1.65	-0.43
Mo	0.107	0.006	-0.009	-3.10	-1.93	-0.26
Ru	0.037	-0.094	-0.027	-1.96	-0.22	0.32
Rh	-0.029	-0.149	-0.034	-0.18	1.07	0.89
Pd	-0.109	-0.192	-0.035	1.07	0.88	1.35
W	0.115	-0.009	-0.006	-3.86	-2.04	-0.92
Re	0.097	-0.041	0.008	-3.27	-1.71	-0.60
Os	0.036	-0.115	-0.015	-2.70	-0.57	0.38
Ir	-0.035	-0.179	-0.025	-1.45	0.33	0.37
Pt	-0.120	-0.211	-0.035	-0.29	0.48	0.75
Au	-0.192	-0.269	-0.039	0.23	0.82	0.72

Figure 2 reproduced from Ref. [14] shows perturbations of the charge (electron) density on the iron nucleus and perturbations of the iron hyperfine field versus relaxed distance r from the impurity. The reference level has been set as the average over 7th till 13th shell excluding 12th shell, as the latter is beyond the super-cell.

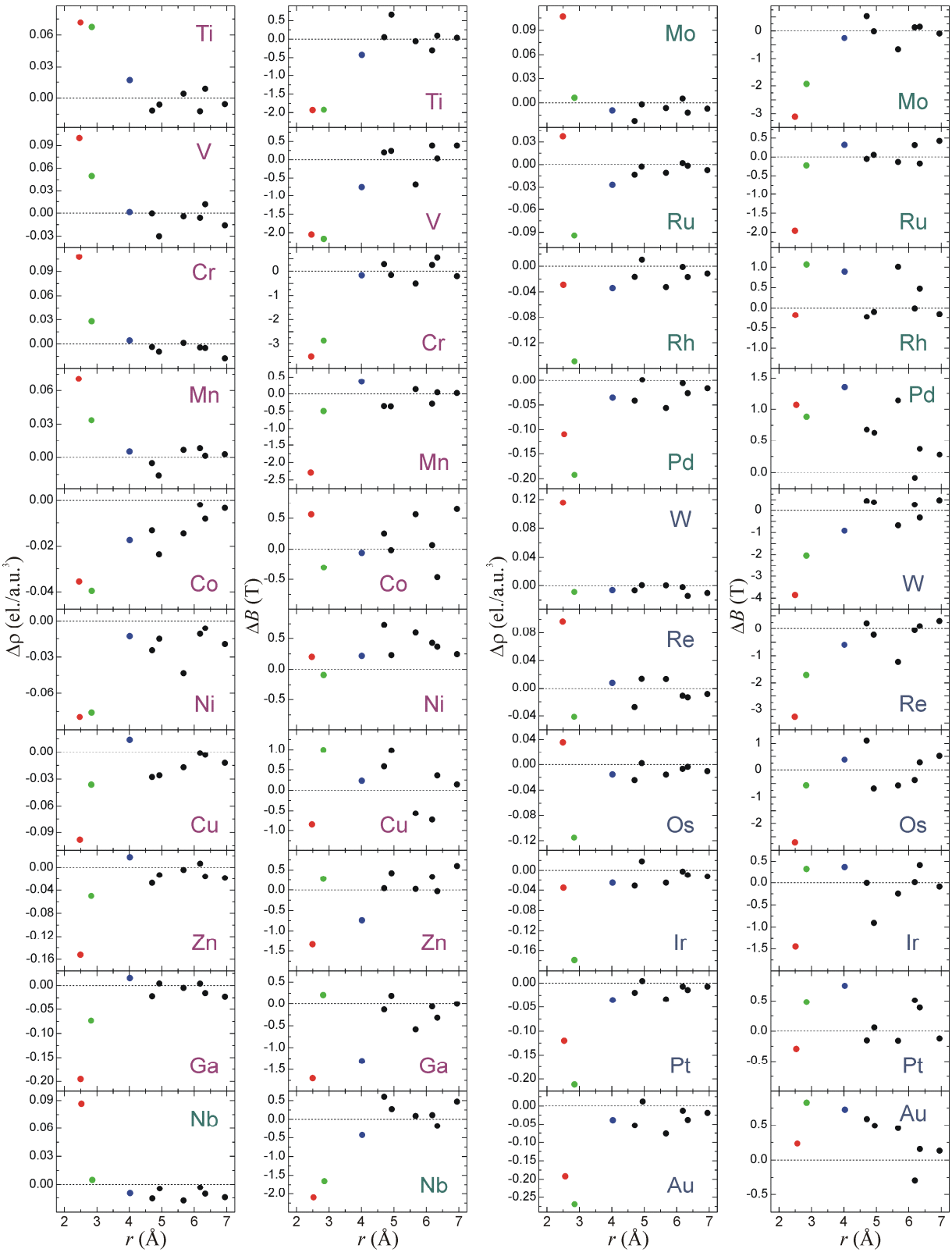

Figure 2 Calculated electron density perturbations $\Delta\rho$ and spin density perturbations ΔB plotted versus relaxed distance r from the impurity for various impurities. The zero level has been determined as described within text. Color distinguishes three first coordination shells. Figure is reproduced from Ref. [14].

Experimental results

The arc melting method was used to prepare alloys. Hence, the alloys remained random alloys except for the extremely low solubility like for the Fe-Cu system [13]. The Fe-Zn system was prepared by the solid state reaction due to the extremely high vapor pressure of zinc at elevated temperatures [13]. Samples were investigated by the X-ray diffraction method and the electron microprobe was used to search for the impurity concentration and global distribution. Some of the specimens contained spurious additional phases at high impurity concentration. The phase separation has been studied in detail for the Fe-Au alloys and the fractal structure has been found between two phases, i.e., the BCC and FCC phase [6]. The fractal structure has been studied applying new algorithm called the roughness method [15, 16]. The roughness method has been designed especially to look upon fractal dimension of the multiple embedded structures leading to the fuzzy and irregular boundaries between objects at a particular level. The phase separation in alloys leads quite often to such patterns.

Absorbers were prepared in the powder form and the spectra were collected at room temperature versus impurity concentration. The following systems Fe-X have been investigated: X = Cu [13], Zn [13], Ga [5], Nb [3], Mo [10], Ru [4], Rh [9], Pd [1], Os [2], Ir [7], Au [6]. Strong oscillations of the spin and charge (electron) density around impurity were found in several cases (see Figure 3) with the strong mixing between outer shells of the impurity and the conduction band [4, 7]. These oscillations have been confirmed by the *ab initio* calculations [14]. Experimental results were used to compare with the results of calculations.

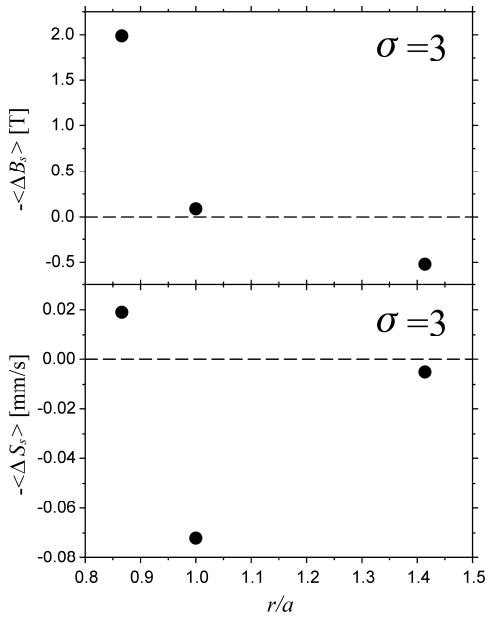

Figure 3 Electron spin density perturbation due to the ruthenium impurity and corresponding electron density perturbation plotted versus relative distance from the mean position of the impurity. Data were averaged over all non-zero ruthenium concentrations investigated. Figure is reproduced from Ref. [4].

The order parameter *s* has been investigated for Fe-Zn and Fe-Cu alloys versus impurity concentration – for details and exact definition of the order parameter see [13]. A plot of the order parameter versus impurity concentration is shown below in Figure 4 reproduced from the Ref. [13].

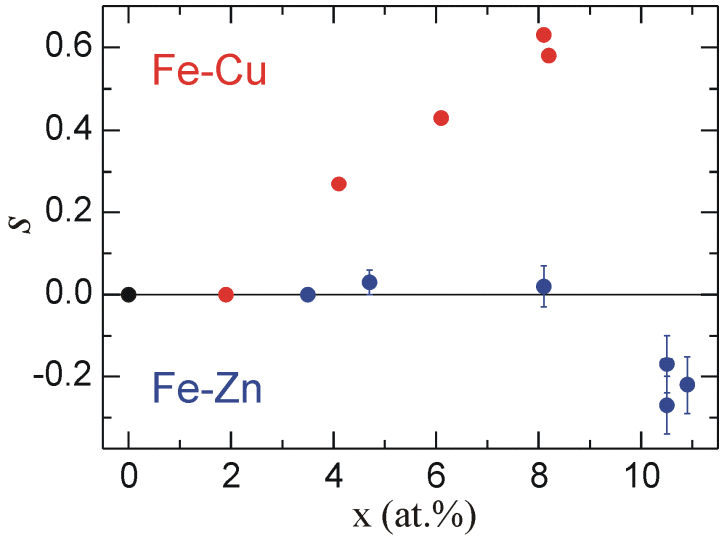

Figure 4 Plot of the order parameter s versus impurity concentration x in the BCC phase of $Fe_{100-x}Cu_x$ and $Fe_{100-x}Zn_x$ alloys. The black dot representing pure α-Fe is shown, too, with the order parameter set to zero by definition. Figure is reproduced from Ref. [13].

One can conclude that zinc atoms try to avoid each other in the α-Fe matrix, while the opposite happens for the copper atoms [13]. It means that Zn-Zn nearest neighbor interaction energy within above structure is much smaller in absolute terms than the Fe-Zn (Zn-Fe) energy. The case of copper is opposite. Hence, the Cu-Cu interaction energy exceeds Fe-Cu (Cu-Fe) coupling energy. These results are consistent with the solubility limits of above elements in the α-Fe.

Future plans and other (selected) activity

I have established scientific cooperation with the scientific establishments in the Czech Republic and Switzerland. Collaboration with the Institute of Physics, Academy of Sciences, Prague, Czech Republic is concerned with the investigations of the intermetallics between iron and rare earths or actinides. A departure from stoichiometry has been established together with the determination of the crystal site occupancy in $R_{2-x}Fe_{14+2x}Si_3$ [17]. The spin reorientation in $Er_{2-x}Fe_{14+2x}Si_3$ has been studied as well [18]. Collaboration with the Laboratory for Solid State Physics, ETH, Zürich, Switzerland is concerned with the investigations of the iron-based superconductors discovered in 2008. Currently efforts are concentrated on the investigations of the iron-based superconductors by means of the Mössbauer spectroscopy. This activity is to be continued for the nearest future. Main results obtained up to now could be briefly summarized as follows. It has been shown by *ab initio* calculations that the ground states of the hexagonal and tetragonal FeSe have almost the same energy. Hence, they transform one into another quite easily leading from the anti-ferromagnetic Mott insulator (hexagonal) into metallic system without magnetic moment. Experimental investigation of the FeSe superconductor has shown that the magnetic moment per chemical formula is much lesser than $0.01\mu_B$ [19]. Hence, all theories basing on the exotic Cooper pairs coupled by the spin fluctuations have been ruled out. Cooper pairs are coupled here by the virtual phonons and remain in the singlet-state. Similar results have been obtained for LiFeP [20]. The parent and doped compounds of the '122' family have been investigated in detail [21, 22]. Very unusual spin density waves (SDW) have been found in parents (orthorhombic structure). They consist of "perforated" magnetized planes ordered in

the b-c plane with the propagation vector and field oriented along the a-axis. The propagation vector is incommensurate with the a lattice constant. The planes are ordered in the anti-ferromagnetic fashion and SDW evolve with the decreasing temperature as narrow magnetized almost to saturation sheets transforming into triangular-like and square-like forms. The "perforation" holes occur in the a-b plane containing separating layers with e.g. Ba, Ca, Eu atoms. The mean squared amplitude of SDW (square root of) behaves according to the (1, 2) universality class versus temperature. It means that one has pure spin-like magnetism following the Ising model with the strong coupling in two dimensions, i.e., in the a-b plane. The incoherent region of SDW is observed above the magnetic transition till the transformation into the tetragonal phase, where the 3d-band magnetism vanishes. The europium magnetism is completely independent i.e. the europium atoms do not see SDW. They order in the anti-ferromagnetic fashion at much lower temperature with the spins oriented along the a-axis. Upon doping one observes rotation of the europium moments onto c-axis with some ferromagnetic component, appearance of the trivalent europium with the transferred field from the divalent europium (local chemical pressure effect), and reduction of SDW strength in somewhat erratic fashion [22]. The mixed state is reached with part of the sample being superconductor without SDW and the remainder still showing SDW. This situation persists to the overdoped region, where SDW definitely vanishes. Divalent europium remains ordered in all these phases. Hence, the 4f magnetism coexists with the superconductivity within the same electronic system. Iron sees transferred field from europium in the doped material, while for parents this field is barely detectable [22], if at all. A transferred field from europium on iron is aligned with the field on divalent europium. It seems that the field on trivalent europium has the same orientation. It has been shown that europium moments remain in the a-c plane without development of any helical structure [22].

References

1. A. Błachowski, K. Ruebenbauer, J. Żukrowski, Effect of Pd impurity on charge and spin density in metallic iron studied by Mössbauer spectroscopy, Physica Scripta **70**(6), 368-373 (2004)
2. A. Błachowski, K. Ruebenbauer, J. Żukrowski, Charge and spin density perturbation on iron atom due to osmium impurity in metallic iron, Nukleonika **49**(Suppl. 3), S67-S70 (2004)
3. A. Błachowski, K. Ruebenbauer, J. Żukrowski, Influence of niobium impurity on spin density in metallic iron, physica status solidi (b) **242**(15), 3201-3208 (2005)
4. A. Błachowski, K. Ruebenbauer, J. Żukrowski, Spin- and charge-density waves around Ru impurities in α-Fe alloys studied by ^{57}Fe Mössbauer spectroscopy, Physical Review B **73**(10), 104423-5 (2006)
5. A. Błachowski, K. Ruebenbauer, J. Żukrowski, J. Przewoźnik, Charge and spin density on iron nuclei in the BCC Fe-Ga alloys studied by Mössbauer spectroscopy, Journal of Alloys and Compounds **455**(1-2), 47-51 (2008)
6. A. Błachowski, K. Ruebenbauer, J. Przewoźnik, J. Żukrowski, Hyperfine interactions on iron nuclei in the BCC and fractally decomposed BCC/FCC mixed phase iron-gold alloys, Journal of Alloys and Compounds **458**(1-2), 96-103 (2008)
7. A. Błachowski, K. Ruebenbauer, J. Żukrowski, Spin- and charge density oscillations around Ir impurity in α-Fe studied by ^{57}Fe Mössbauer spectroscopy, Journal of Alloys and Compounds **464**(1-2), 13-17 (2008)
8. A. Błachowski, Charge and spin density perturbation on iron nuclei by non-magnetic impurities substituted on the iron sites in α-Fe, Acta Physica Polonica A **114**(6), 1563-1571 (2008)

9. A. Błachowski, K. Ruebenbauer, J. Żukrowski, Spin- and charge density around Rh impurity in α-Fe studied by ^{57}Fe Mössbauer spectroscopy, Journal of Alloys and Compounds **477**(1-2), 4-7 (2009)
10. A. Błachowski, K. Ruebenbauer, J. Żukrowski, J. Przewoźnik, Spin and charge density on iron nuclei in the BCC Fe-Mo alloys studied by ^{57}Fe Mössbauer spectroscopy, Journal of Alloys and Compounds **482**(1-2), 23-27 (2009)
11. A. Błachowski, U.D. Wdowik, K. Ruebenbauer, Volume effect and electron band modification in α-Fe by substitutional impurities, Journal of Alloys and Compounds **485**(1-2), 36-40 (2009)
12. A. Błachowski, U.D. Wdowik, Impurity effect on charge and spin density in α-Fe – comparison between cellular model, ab initio calculations and experiment, Acta Physica Polonica A **119**(1), 24-27 (2011)
13. A. Błachowski, K. Ruebenbauer, J. Żukrowski, J. Przewoźnik, J. Marzec, A. Rakowska, Spin- and charge density perturbations and short-range order in Fe-Cu and Fe-Zn BCC alloys: A Mössbauer study, Journal of Physics and Chemistry of Solids **72**(12), 1537-1542 (2011)
14. A. Błachowski, U.D. Wdowik, Transition metal impurity effect on charge and spin density in iron: *Ab initio* calculations and comparison with Mössbauer data, Journal of Physics and Chemistry of Solids, doi:10.1016/j.jpcs.2011.10.017 (2011)

15. A. Błachowski, K. Ruebenbauer, Roughness method to estimate fractal dimension, Acta Physica Polonica A **115**(3), 636-640 (2009)
16. A. Błachowski, K. Ruebenbauer, A. Rakowska, S. Kąc, Fractal-like behaviour of the BCC/FCC phase separation in the iron-gold alloys, Journal of Microscopy **237**(3), 395-398 (2010)
17. A. Błachowski, K. Ruebenbauer, J. Przewoźnik, J. Żukrowski, D. Sitko, N.-T. H. Kim-Ngan, A.V. Andreev, Hyperfine interactions on iron in $R_{2-x}Fe_{14+2x}Si_3$ (R= Ce, Nd, Gd, Dy, Ho, Er, Lu, Y) compounds studied by Mössbauer spectroscopy, Journal of Alloys and Compounds **466**(1-2), 45-51 (2008)
18. J. Żukrowski, A. Błachowski, K. Ruebenbauer, J. Przewoźnik, D. Sitko, N.-T. H. Kim-Ngan, Z. Tarnawski, A.V. Andreev, Spin reorientation in the $Er_{2-x}Fe_{14+2x}Si_3$ single-crystal studied by the ^{57}Fe Mössbauer spectroscopy and magnetic measurements, Journal of Applied Physics **103**(12), 123910-8 (2008)
19. A. Błachowski, K. Ruebenbauer, J. Żukrowski, J. Przewoźnik, K. Wojciechowski, Z. M. Stadnik, Mössbauer spectroscopy evidence for the lack of iron magnetic moment in superconducting FeSe, Journal of Alloys and Compounds **494**(1-2), 1-4 (2010)
20. A. Błachowski, K. Ruebenbauer, J. Żukrowski, J. Przewoźnik, J. Marzec, Mössbauer and magnetic measurements of superconducting LiFeP, Journal of Alloys and Compounds **505**(2), L35-L37 (2010)
21. A. Błachowski, K. Ruebenbauer, J. Żukrowski, K. Rogacki, Z. Bukowski, J. Karpinski, Shape of spin density wave versus temperature in AFe_2As_2 (A = Ca, Ba, Eu): A Mössbauer study, Physical Review B **83**(13), 134410 (2011)
22. A. Błachowski, K. Ruebenbauer, J. Żukrowski, Z. Bukowski, K. Rogacki, P. J. W. Moll, J. Karpinski, Interplay between magnetism and superconductivity in $EuFe_{2-x}Co_xAs_2$ studied by ^{57}Fe and ^{151}Eu Mössbauer spectroscopy, Physical Review B **84**(17), 174503 (2011)

Błachowski